

# Modeling of grid-connected converter-based sources as equivalent impedances for symmetrical and asymmetrical short-circuit calculation

Herick Talles Queiroz Lemos <sup>[1]</sup>, Adriano Aron Freitas de Moura <sup>[2]</sup>, Antônio Marcos Fernandes Filho <sup>[3]</sup>, Ednardo Pereira da Rocha <sup>[4]</sup>, Ailson Pereira de Moura <sup>[5]</sup>

[1] herick.lemos@ufersa.edu.br. [2] adrianoaron@ufersa.edu.br. Universidade Federal Rural do Semi-Árido, Departamento de Engenharia e Tecnologia. [3] antonio.filho@ifce.edu.br. Instituto Federal de Educação Ciência e Tecnologia do Ceará. [4] ednardo.pereira@ufersa.edu.br. Universidade Federal Rural do Semi-Árido, Departamento de Engenharia e Tecnologia. [5] ailson@ufc.br. Universidade Federal do Ceará, Departamento de Engenharia Elétrica.

## ABSTRACT

The study of electrical systems under fault conditions provides fundamental information for proper system protection design and coordination. These studies are traditionally performed in the phasor domain and based on the physical behavior of the synchronous generators directly connected to the grid. However, the increase of converter-based renewable sources (CBRSs) connections to the grid have created the need for new short-circuit (SC) calculation methods, since, unlike the synchronous generators, the converter SC contribution depends only on its Fault Ride Through (FRT) and active power injection requirements. In this paper, a comprehensive approach for steady-state SC calculation in power systems with CBRSs is proposed. The proposed approach is based on the bus impedance matrix and can be used for symmetrical and asymmetrical SC calculation considering both positive and negative sequence currents from converters as required in the grid codes of many countries. The proposed approach is demonstrated with a 17-bus test system containing converter-controlled photovoltaic (PV) and wind generation submitted to the Brazilian Electric Grid code requirements. By comparing the obtained results with the grid code requirements, the effectiveness of the proposed iterative approach in the estimation of the steady-state SC current contribution from CBRSs is verified.

**Keywords:** Short-circuit analysis. Full-scale converters. Distributed generation. Type IV wind turbine. Photovoltaic generators.

## RESUMO

*O estudo dos sistemas elétricos em condições de falta fornece informações fundamentais para o projeto e a coordenação adequada da proteção do sistema. Esses estudos são realizados, tradicionalmente, no domínio fasorial e com base no comportamento físico dos geradores síncronos diretamente conectados à rede. No entanto, com o aumento das conexões à rede de fontes renováveis via conversores de frequência, surge a necessidade do desenvolvimento de novos métodos de cálculo de curto-circuito (SC), pois, diferentemente dos geradores síncronos, a contribuição do conversor para o SC depende apenas de sua estratégia de FRT (Fault Ride Through - FRT) e dos requisitos de injeção de energia ativa. Neste artigo, uma abordagem geral para o cálculo de SCs em regime permanente em sistemas de energia com fontes renováveis acopladas à rede via conversores de frequência completos (CBRSs) é proposta. Essa abordagem é baseada na matriz de impedância de barra e pode ser usada para o cálculo de SCs simétricos e assimétricos, considerando as correntes de sequência positiva e negativa dos conversores, conforme exigido nos códigos de rede de muitos países. A abordagem proposta é demonstrada com um sistema de 17 barras contendo geradores fotovoltaicos (PV) controlados por conversor e geração eólica, ambos submetidos aos requisitos do código da Rede Elétrica Brasileira. Ao comparar os resultados obtidos com os requisitos do código de rede, constatou-se a eficácia da abordagem iterativa proposta na estimativa da contribuição para o SC em regime permanente de CBRSs.*

**Palavras-chave:** Análise de curtos-circuitos. Conversores completos. Geração distribuída. Turbinas eólicas tipo IV. Geradores fotovoltaicos.

Nomenclature			
APC	Active power control	$I_{C,s+}^{r*}$	Reactive current reference for positive sequence
CBRS	Converter-based renewable source	$I_{C,s-}^{a*}$	Active current reference for negative sequence
FRT	Fault Ride Through	$I_{C,s-}^{r*}$	Reactive current reference for negative sequence
GSU	Grid side DC/AC converter	$P_{s+}$	Positive sequence active power contribution
LG	Single line-to-ground fault	$P_{s-}$	Negative sequence active power contribution
LL	Line-to-line fault	$Q_{s+}$	Positive sequence reactive power contribution
LLG	Double line-to-ground fault	$Q_{s-}$	Negative sequence reactive power contribution
LLL	Three-phase fault	$V_n$	Nominal voltage
LLLG	Three-phase-to-ground fault	$V_{s+}$	Positive sequence voltage
P	Active power	$V_{C,s+}$	Converter positive sequence voltage
PGU	Power generation unit	$V_{C,s-}$	Converter negative sequence voltage
PV	Photovoltaic	$Z_{C,s+}$	Converter positive sequence impedance
Q	Reactive power	$Z_{C,s-}$	Converter negative sequence impedance
SC	Short-circuit	$Z_f$	Fault impedance
WT	Wind turbine	$\epsilon_I$	Error tolerance for current magnitude
$I_{s+}$	Positive sequence current contribution	$\epsilon_\theta$	Error tolerance for current angle
$I_{s-}$	Negative sequence current contribution	$\epsilon_I^{max}$	Absolute maximum error for current magnitude
$I_{C,s+}^*$	Current reference for positive sequence	$\epsilon_\theta^{max}$	Absolute maximum error for current angle
$I_{C,s-}^*$	Current reference for negative sequence	$\Delta I_{s+}^r$	Additional reactive current injection in positive sequence
$I_{C,s+}^{a*}$	Active current reference for positive sequence		

## 1 Introduction

The occurrence of disturbances in electrical power systems poses serious risks to the safety and normality of its operational state. Such disturbances cause changes in electrical magnitudes and, often, violations of operational restrictions, which creates the need for corrective actions to reduce or mitigate the consequences of these disturbances.

The most common and the most severe disturbances are the short-circuits or shunt faults, which are associated with faults in equipment insulation, surges caused by lightning strikes or circuit

switching, climatic adversities and other mechanical causes. By frequency of occurrence, the most common type of shunt fault is the single line-to-ground (LG) fault with 70% of occurrences, followed by line-to-line (LL), double line-to-ground (LLG) and three-phase (LLL) faults, which correspond to 15%, 10% and 5% of occurrences, respectively (ANDERSON, 1995).

In power systems based on synchronous machines, the resulting fault current magnitude depends on the internal voltage of the machines and the impedances between these machines and the fault location. This fault current is generally much higher than the operating current of the system and,

if not interrupted, can cause irreparable thermal and mechanical damage to the system components.

In this sense, fault analysis is an important part of the power systems analysis, since the information gained from this analysis allows, among other things, the determination of the circuit breakers and fuses interruption capacity, protection relays settings and their coordination with other protection devices, and cable thermal and mechanical ratings.

With the increase in the integration of grid-connected converter-based renewable sources, the utilities have been forced to revise grid codes requirements in order to account for the impact from such units in the power system stability and fault level. Unlike synchronous generators, during a fault, the converter-based units inject controlled currents to the grid that are defined by the grid code requirements and have magnitudes limited to the converter ratings. Consequently, converter-based sources cannot be properly modeled in classical short-circuit (SC) calculation methods (TLEIS, 2007).

In the past few years, several studies have been conducted with the aim of developing new SC calculation methods capable of representing the controlled behavior of the current contribution from the converters to evaluate the real impact of this contribution on the planning and operation of energy systems.

In Valentini *et al* (2008), type IV wind turbines (WTs) are modeled as current sources with magnitude set at 1 pu and phase angle adjusted according to the voltage support requirements of German E.ON Netz grid code. In Walling, Gursay and English (2012), it is proposed a phasor approach where the active and reactive current injection of type IV WTs is obtained in look-up tables provided by the manufacturers and created as a function of the terminal voltage of the machine for a certain instant after the fault.

In Fischer and Mendonça (2011), Enercon type IV WTs are also represented as a voltage source behind a variable impedance that injects only positive sequence currents with fixed magnitude at the maximum converter output current and phase angle of 90 degrees. In Chen *et al* (2012), the converter-based renewable sources are modeled for symmetric faults as voltage sources behind a variable reactance iteratively adjusted to provide the reactive current defined by the Danish grid code.

In Moura *et al* (2015), a novel fault method is proposed based on the inverter matrix impedance

(IMI) and impedance-current vector (ICV) where PV generators are modeled as constant power sources that contribute only with positive sequence currents. In Kauffmann *et al* (2015), it is proposed a phasor approach to symmetric fault analysis where type IV WTs and the network are modeled using the Modified Augmentation Nodal Analysis (MANA) technique, which requires the use of LU factorization algorithms to solve the network equations. In Göksu *et al* (2016), it is suggested an iterative approach for the analysis of symmetric and asymmetric faults using the bus admittance matrix.

As shown previously, most existing solutions for SC calculation in power systems with converter-controlled sources are limited to the calculation of symmetric faults or, when extended for asymmetric faults, require the use of bus admittance matrix (or its augmented version), which is not a reasonable choice for handling distribution systems as the admittance matrix may become singular or near-singular which need special numerical techniques.

In this research, a comprehensive approach for steady-state SC calculation in power systems with converter-based renewable sources is proposed. The proposed approach is based on the bus impedance matrix and can be used for symmetrical and asymmetrical SC calculation considering both positive and negative sequence currents from converters as required in the Transmission System Operator grid code.

This paper is organized as follows: section 2 discusses the behavior of the converter-based generator under fault conditions and presents the model used for its representation in the SC calculation; section 3 presents in detail the proposed iterative approach; section 4 presents a numerical demonstration of the proposed approach using a 17-bus test system; section 5 concludes the study.

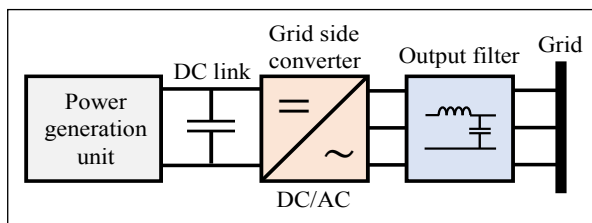
## 2 Converter-based renewable sources

With the growing worldwide effort to decarbonize electric power generation, a wide variety of generation plant types have been connected to distribution and transmission power grids. Examples are the well-established combined heat and power (CHP)

technologies, wind turbines and photovoltaic systems. In addition to these, there are many new technologies such as fuel cells, heliothermic plants, micro CHPs, flywheels and flow batteries, which are at different levels of demonstration of their economic viability (JENKINS; EKANAYKE; STRBAC, 2010).

Many distributed renewable energy sources use power electronics converters as the interface to the network. In these units, the main objectives of the converters are conditioning the generator produced energy to meet the grid requirements and to maximize the extraction of the energy source (BOLLEN; HASSAN, 2011). Figure 1 illustrates the main components of a typical converter-based source.

**Figure 1** – Main components of a typical converter-based source



Source: authors.

The converter power generation unit (PGU) converts to DC the power produced by the generator (fuel cells, WT or PV) and delivered it to the DC link. Power conversion in the PGU can be done by means of a DC/DC converter (buck-boost) or an AC/DC converter (full-bridge rectifier) depending on the generation source. In this unit, the main objective of the control system is to maximize power extraction from the source (ABDALRAHMAN; ZEKRY; ALSHAZLY, 2012).

The DC link voltage is applied to the grid side DC/AC converter (GSC), which is responsible for controlling the active and reactive power output and grid synchronization. An LC or LCL filter is connected between the GSC output and grid to reduce the harmonic content (BOLLEN; HASSAN, 2011). The DC link gives the GSC the ability to control the output power independently of the input power in the PGU (BARSCH *et al*, 2012). In other words, the electrical output of the converter-based source is completely defined by the hardware and firmware used in the GSC.

Under fault conditions, the current contribution from the converter is dependent on the pre-fault GSC control strategy and the FRT (Fault Ride Through) requirements. Unlike synchronous generators whose SC current contribution can exceed 10 pu (PLET *et al*,

2012) and has behavior a described from three well-defined time periods (sub-transient, transient and steady-state regimes), the converter-based generators are limited to peak currents up to 3 pu (WALLING; GURSAY; ENGLISH, 2012) that are described by only two periods: the instants that precede the fault detection, 1 to 2 cycles; and the period after the fault detection (BARSCH *et al*, 2012), in which the FRT control strategy is applied.

Another important feature of the GSC is the capability to control their fault current contribution independently in the active and reactive components for both positive and negative sequences. In the case of ground faults, the zero-sequence current injection generally suppressed by GSC (NELSON, 2012). In addition, the converter-based unit is commonly interconnected to the grid by delta-star-connected step-up transformers, which isolate the GSC from the zero-sequence network (VAN DE SANDT *et al* 2009; GÖKSU *et al*, 2016).

## 2.1 FRT requirements and active power injection

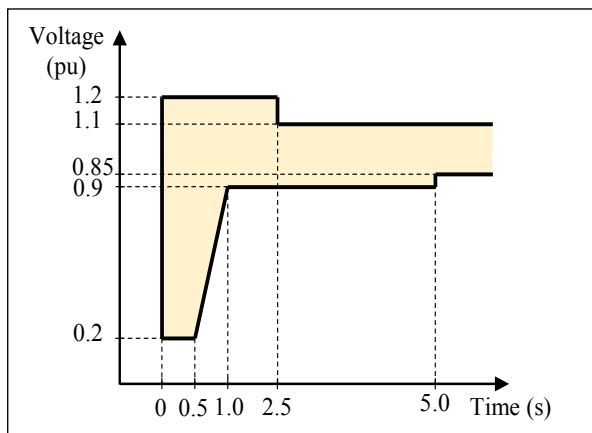
The growth in installed capacity of grid-connected renewable sources has led the transmission system operators to update the applicable grid codes with specific technical requirements to address the integration impacts on grid stability and power quality. In recent grid codes, renewables generation units as PV and WTs, are expected to stay connected to the grid during a time period that depends on the voltage drop in the generator terminals and provides support the positive sequence grid voltage by injecting reactive currents during the SC, for both symmetrical and asymmetrical faults.

Figure 2 illustrates the Brazilian grid code supportability requirement for dynamic under and overvoltage due to disturbances in the electrical grid. According to this requirement, wind or photovoltaic power plants must continue to operate if the voltage at the WT or PV inverter terminals remains within the region indicated in Figure 2.

In addition to the requirement of Figure 2, the Brazilian grid code also requires that WTs and PV plants be able to provide voltage support to the grid through the injection of additional reactive current ( $\Delta I_{s+}^r$ ) for positive sequence voltages ( $V_{s+}$ ) below 85%, and reactive current consumption for voltages above 110% of the converter rated voltage, as shown in Figure 3. In certain countries' grid codes, it is also common to use as a voltage reference (commonly referred to as the feedback voltage) for application of this requirement the bus voltage on the low voltage side of the unit step-up transformers.

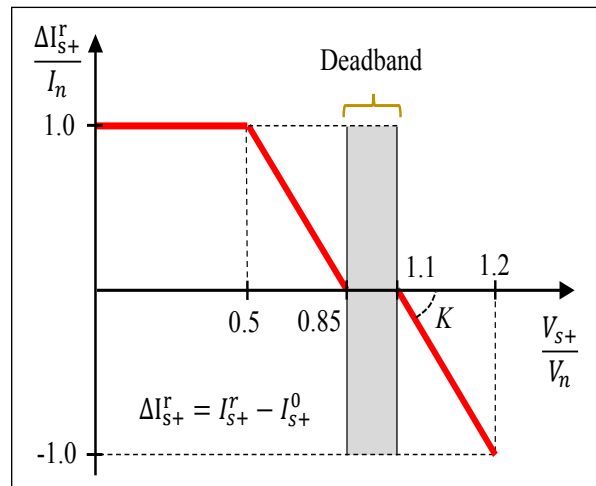
Another important grid code requirement is the active power injection control during small voltage variations in the electrical network. This requirement prevents the occurrence of system instabilities such as voltage collapses as a function of the active power injection deficit created with the disconnection of the generators by undervoltage as well as ensures that the power injected from generators into the grid has an acceptable power factor. Figure 4 illustrates Brazilian grid code requirements for active power injection into the grid. In Figure 4,  $Q$  and  $P_{\text{m\acute{a}x}}$  are the CBRS reactive and maximum active output power, respectively, and  $V_{PCC}$  is its voltage at the point of common coupling.

**Figure 2** – Brazilian grid code supportability requirement for dynamic under and overvoltage



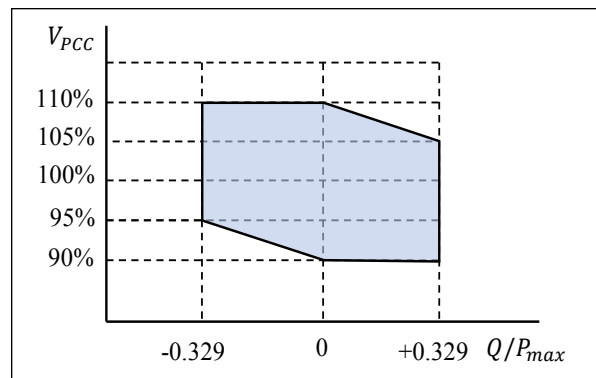
Source: Adapted from OPERADOR NACIONAL DO SISTEMA ELÉTRICO (2019).

**Figure 3** – Brazilian grid code requirement for grid voltage support



Source: Adapted from OPERADOR NACIONAL DO SISTEMA ELÉTRICO (2019).

**Figure 4** – Brazilian grid code requirement for active power injection



Source: Adapted from OPERADOR NACIONAL DO SISTEMA ELÉTRICO (2019).

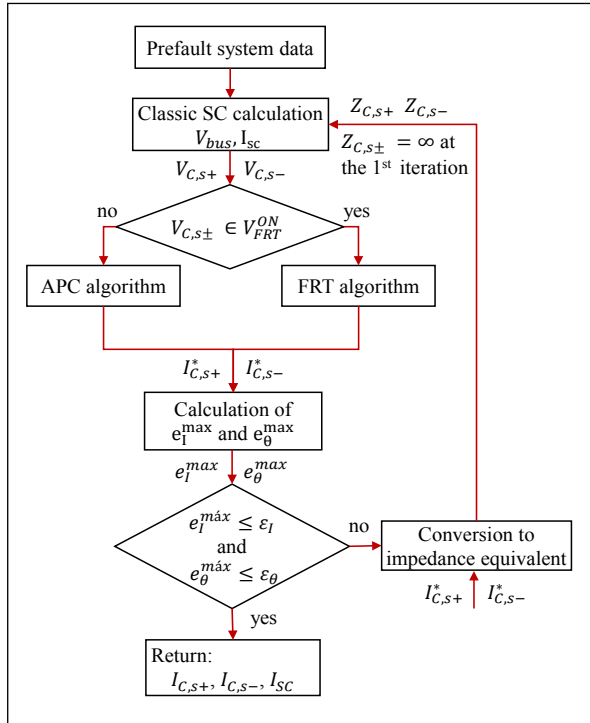
### 3 Proposed iterative approach

An iterative approach can be used to estimate the steady-state SC contribution from converter-based generators. The idea is to iteratively adjust the SC contributions from the converter-controlled units to match the specific grid code requirements to voltage reinforcements and active power injection on voltage dips. To perform the SC calculation, the network's positive negative and zero sequence impedance matrices are required as well as the converter's pre-fault power injections.

In Figure 5 the proposed iterative approach's block diagram is shown. The iterative SC calculation starts with the loading of the network's pre-fault data. The

bus voltages and active and reactive power injected by the converters can be obtained by load flow analysis or, alternatively, fixed at 1 pu and the converters maximum power ratings respectively.

Figure 5 – Iterative approach block diagram to SC calculation



In the “SC calculation” block the bus sequence voltages ( $V_{bus}$ ) and SC current ( $I_{sc}$ ) are calculated by the classic SC method using the bus impedance matrix and Thevenin’s and Superposition Theorem at every iteration for the faulted network.

For the first algorithm iteration, all converter-based renewable sources (CBRS) current magnitudes are set to zero which, in other words, implies that its impedance equivalents are infinite at the first iteration. For the other iterations, the SC current contributions in the positive and negative sequence for a given converter are calculated by:

$$I_{C,s+} = \frac{1 - V_{C,s+}}{Z_{C,s+}} \quad (1)$$

$$I_{C,s-} = \frac{1 - V_{C,s-}}{Z_{C,s-}} \quad (2)$$

where  $I_{C,s±}$  and  $V_{C,s±}$  are the converter’s current contribution and voltages in the positive and negative

sequence, respectively, and  $Z_{C,s+}$  and  $Z_{C,s-}$  are the converter’s impedance equivalents in the positive and negative sequence, respectively.

From the output of “SC calculation” block, the voltages of the converters’ feedback buses are obtained. If the feedback bus voltage of a given converter is within the FRT control operating range ( $V_{FRT}^{ON}$ ), the “FRT algorithm” block is switch on to create the active and reactive current reference in positive ( $I_{C,s+}^{a,*}$ ,  $I_{C,s+}^{r,*}$ ) and negative ( $I_{C,s-}^{a,*}$ ,  $I_{C,s-}^{r,*}$ ) sequence components. Otherwise, the “APC algorithm” block switches on to create the active current reference ( $I_{C,s+}^{a,*}$ ) by means of an active power control (APC) algorithm.

When in the FRT control mode, the reactive current references in the positive and negative sequences are generated according to the voltage support requirements and active and reactive currents references in the positive and negative sequences are generated in order to maintain the active output power of the converter constant.

By applying symmetrical components theory, the per-unit active ( $P$ ) and reactive ( $Q$ ) output power of the converter is given by:

$$P = P_{s+} + P_{s-} \quad (3)$$

$$Q = Q_{s+} + Q_{s-} \quad (4)$$

where  $P_{s+}$ ,  $P_{s-}$ ,  $Q_{s+}$  and  $Q_{s-}$  are the positive and negative sequence contributions to the active and reactive output power respectively, and which are computed using (5)-(8):

$$P_{s+} = V_{C,s+} \overline{I_{C,s+}^{a,*}} \quad (5)$$

$$P_{s-} = V_{C,s-} \overline{I_{C,s-}^{a,*}} \quad (6)$$

$$Q_{s+} = V_{C,s+} \overline{I_{C,s+}^{r,*}} \quad (7)$$

$$Q_{s-} = V_{C,s-} \overline{I_{C,s-}^{r,*}} \quad (8)$$

Since the purpose of the negative sequence current injection is to reduce the negative sequence grid voltage by injection of  $Q_{s-}$ , the term  $P_{s-}$  can be set to zero, so that the active current reference in the positive sequence can be determined (7) as:

$$I_{C,s+}^{a,*} = \frac{P}{V_{C,s+}} \quad (9)$$

At the first iteration,  $P$  is set to its pre-fault value. However, if during the iterative process the current

in any phase exceeds the converter maximum output current ( $I_{max}$ ), the active power must be reduced to give priority to the reactive current injection.

When in APC mode,  $Q$  is held constant while the active current reference in the positive sequence is calculated by Equation 9 in order to adjust  $P$  to its pre-fault value. For the  $i$ -th iteration, the active power to be injected is determined by:

$$P^{(i)} = P^{(i-1)} + k_p(P_0 - P^{(i-1)}) \quad (10)$$

where  $k_p$  is a positive constant less than 1 and  $P_0$  is the pre-fault active power injected by the converter into the grid. During the iterative process, if the current in any phase exceeds  $I_{max}$ , the active power must be reduced to give priority to the reactive power injection. This procedure avoids that the increase of  $P$  due to the reduction of  $Q$  causes a voltage drop in the feedback buses, which may require a new reactive power adjust in the "FRT algorithm" block.

The reference currents generated for each sequence are used to calculate the magnitude and phase errors in relation to the SC current contributions obtained for the converters in the "SC calculation" block. The magnitude and phase errors as calculated as follows:

$$e_{I+} = |I_{C,s+}^*| - |I_{C,s+}| \quad (11)$$

$$e_{I-} = |I_{C,s-}^*| - |I_{C,s-}| \quad (12)$$

$$e_{\theta+} = \angle I_{C,s+}^* - \angle I_{C,s+} \quad (13)$$

$$e_{\theta-} = \angle I_{C,s-}^* - \angle I_{C,s-} \quad (14)$$

$$e_I^{max} = \max(|e_{I+}|, |e_{I-}|) \quad (15)$$

$$e_{\theta}^{max} = \max(|e_{\theta+}|, |e_{\theta-}|) \quad (16)$$

The magnitude errors ( $e_{I+}$ ,  $e_{I-}$ ) defined in (11) and (12) and the angle errors ( $e_{\theta+}$ ,  $e_{\theta-}$ ) defined in (13) and (14) are the differences between the reference magnitudes and angles obtained for positive and negative sequences currents and its corresponding values obtained in "SC calculation" block by means of the (1) and (2). In Equations 13 and 14 the absolute maximum values calculated for magnitude ( $e_I^{max}$ ,  $e_{\theta}^{max}$ ) and angle errors are obtained respectively.

After the error's calculations, the obtained values for  $e_I^{max}$  and  $e_{\theta}^{max}$  are compared with the defined

error limits for magnitude ( $\epsilon_I$ ) and angle ( $\epsilon_{\theta}$ ). If the errors are less than or equal to the defined error limits, the iterative process is ended, and SC calculations results are returned, i.e. the phasor solution of the faulted network including the converters' positive and negative sequence current contributions.

However, if the errors are greater than the defined error limits, the reference currents generated for each sequence are used to calculate the converters' impedance equivalents used in the next iteration. In the  $i$ th iteration, for example, the new impedance equivalent of a given CBRS is obtained by:

$$Z_{C,s+}^{(i+1)} = \frac{1 - V_{C,s+}^{(i)}}{I_{C,s+}^{*(i)}} \quad (17)$$

$$Z_{C,s-}^{(i+1)} = \frac{1 - V_{C,s-}^{(i)}}{I_{C,s-}^{*(i)}} \quad (18)$$

$$Z_{C,s}^{(i+1)} = \begin{bmatrix} \infty & 0 & 0 \\ 0 & Z_{C,s+}^{(i+1)} & 0 \\ 0 & 0 & Z_{C,s-}^{(i+1)} \end{bmatrix} \quad (19)$$

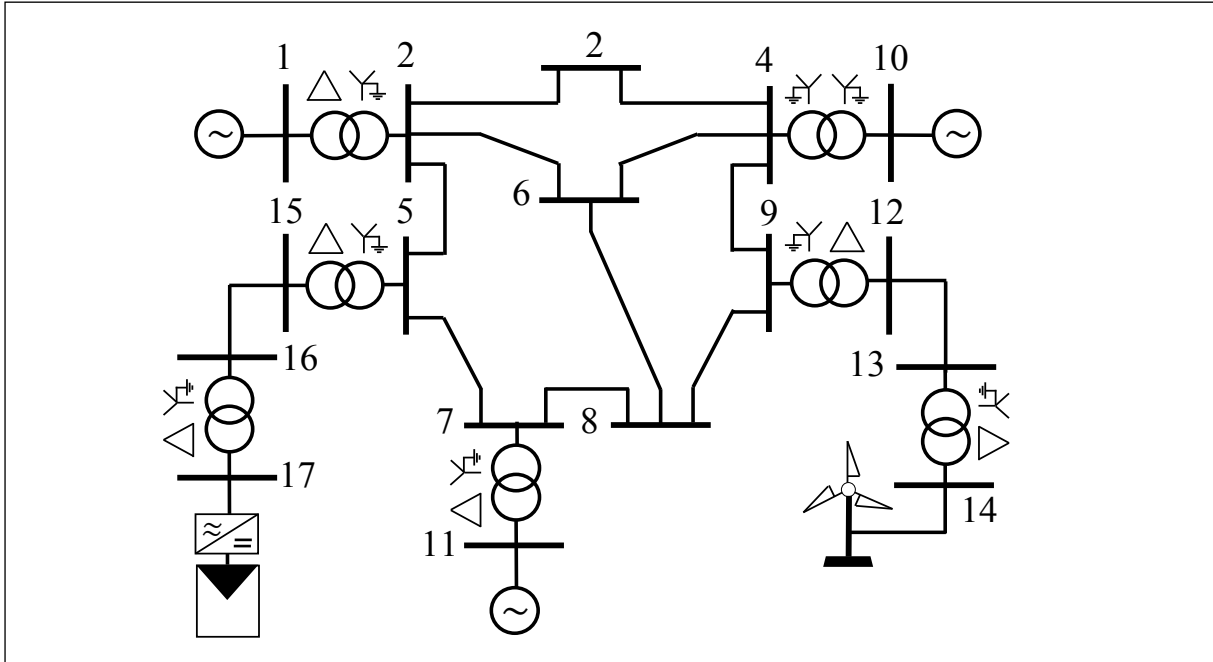
The described iterative approach is executed until all converters' magnitudes and angles converge for both positive and negative sequences. At the end of the iterative process, the results of the faulted network can be used to evaluate the impact of the converters' SC contribution to the network protection and coordination.

## 4 Demonstration example

In this section, the proposed iterative approach is demonstrated with a network containing converter-controlled PV and wind generation. The network topology is shown in Figure 6. All network impedances values in pu and base values as well the converters ratings are given in the Appendix.

The PV generator was connected to bus 17 and has the pre-fault active power injection of 0.015 pu (rated power) with unity power factor and maximum output current of 0.0195 pu (1.3 times its rated current). The WT was connected to bus 14 and has the pre-fault active power injection of 0.025 pu (rated power) with unity power factor and maximum output current of 0.0325 pu (1.3 times its rated current). For both PV and WT, the feedback voltages were collected in their own connection buses with the network, i.e. the busses 17 and 14, respectively.

Figure 6 – 17 bus test systems used in the demonstration example



In the demonstration example, the LG, LL, LLG, LLL, and LLLG (three-phase-to-ground) faults were evaluated on bus 6. The fault impedance ( $Z_f$ ) values were specifically chosen to illustrate the performance of the converters in the FRT and APC control modes. The FRT and APC requirements of the Brazilian grid code were used. For the positive sequence, the proportional factors  $K$  and  $k_P$  were set as 2 and 0.1 respectively. Since there is no negative sequence requirement in the Brazilian grid code, the negative sequence current was omitted and not included in the iterative SC calculations. The convergence error limit

for the current magnitude ( $\epsilon_\theta$ ) and current angle ( $\epsilon_I$ ) was set as  $\Delta I_{S+}^{r,*}$ . The network and proposed iterative SC calculation were implemented in MATLAB®.

Tables 1 and 2 summarize results for the feedback bus voltage, fault current contribution, and active and reactive power injection from PV and wind generators. For used error limits, the maximum iterations number required was 51 iterations (LLG fault). In the simulations, it was found that the FRT mode requires a larger number of iterations as is especially small when the feedback voltage is close to 0.85 pu (upper limit of the FRT operation control for reactive consumption).

Table 1 – WT fault results – bus 6

Fault type (phase)	$Z_f (\Omega)$	Positive sequence voltage (pu)	Positive sequence current contribution (pu)	$P$ (pu)	$Q$ (pu)	Power factor
LG (a)	100	0.8969–0.5323°	0.0279–0.5323°	0.0250	0.0000	1.0000
LL (a-b)	10	0.8060–1.1553°	0.0325–91.1553°	0.0000	0.0262	0.0000
LLG (a-b)	150	0.7867–2.7869°	0.0325–92.7869°	0.0000	0.0256	0.0000
LLL	0	0.5413–0.7941°	0.0325–90.7941°	0.0000	0.0176	0.0000
LLLG	150	0.8500–15.3099°	0.0325–73.4276°	0.0146	0.0235	0.5282 ind.



**Table 2** – PV fault results – bus 6

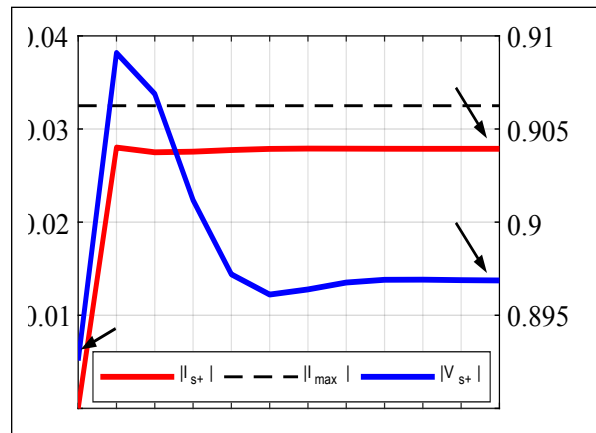
Fault type (phase)	$Z_f (\Omega)$	Positive sequence voltage (pu)	Positive sequence current contribution (pu)	$P$ (pu)	$Q$ (pu)	Power factor
LG (a)	100	0.9323–0.6491°	0.0161–0.6491°	0.0150	0.0000	1.0000
LL (a-b)	10	0.85001.8079°	0.0194–22.6252°	0.0150	0.0068	0.9104 ind.
LLG (a-b)	150	0.85000.1108°	0.0195–50.8448°	0.0104	0.0129	0.6299 ind.
LLL	0	0.6963–0.3355°	0.0195–90.3355°	0.0000	0.0136	0.0000
LLLG	150	0.8583–8.1690°	0.0175–8.1690°	0.0150	0.0000	1.0000

For all analyzed faults, it was verified that the results obtained correspond exactly with the expected response for the converter according to the applied grid requirements. For the LG fault, for example, the feedback voltages of both PV and WT generators are in the deadband of the FRT control, so that the current control during the fault was the APC, which was able to maintain the active and reactive power injections in their pre-fault values. Figures 7 and 8 illustrate the algorithm responsible for the LG fault during the iterative process.

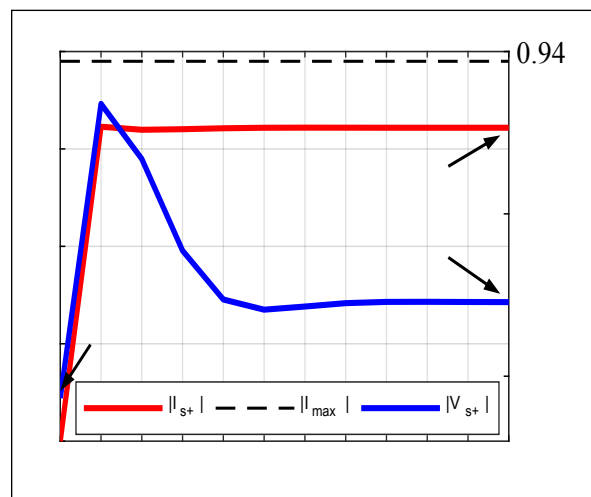
Figure 7 shows that the PV and WT currents are set to zero in the first iteration, which results in the feedback voltages (without voltage support) of  $0.8969\angle-0.5323^\circ$  pu and  $0.8926\angle-4.3043^\circ$  pu for the PV and WT, respectively. In the second iteration, the PV and WT currents are adjusted according to the APC control mode. The convergence criterion is satisfied in the 12th iteration, in which the currents of  $0.0279\angle-0.5323^\circ$  pu and  $0.0161\angle-0.6491^\circ$  pu and feedback voltages of  $0.8969\angle-0.5323^\circ$  pu and  $0.9323\angle-0.6491^\circ$  pu are observed for the PV and WT, respectively. Both WT and PV current contributions do not exceed their maximum nominal values.

In Figure 8, it is observed that the APC control correctly adjusts the converters' active power from 0 pu (first iteration) to its pre-fault values, i.e. 0.0250 pu for the PV and 0.0150 pu for the WT, both with unity power factor. The reactive power injection verified in the first iterations originates in the phase angle error between the reference current generated by the APC control and the current effectively injected by the converter (obtained in the SC calculation).

**Figure 7** – WT (a) and PV (b) positive sequence current contributions and feedback bus voltages for L-G ( $Z_f=10\Omega$ ) fault at bus 6



(a)



(b)

Figure 8 – WT (a) and PV(b) active and reactive power injections for an L-G ( $Z_f=100\Omega$ ) fault at bus 6

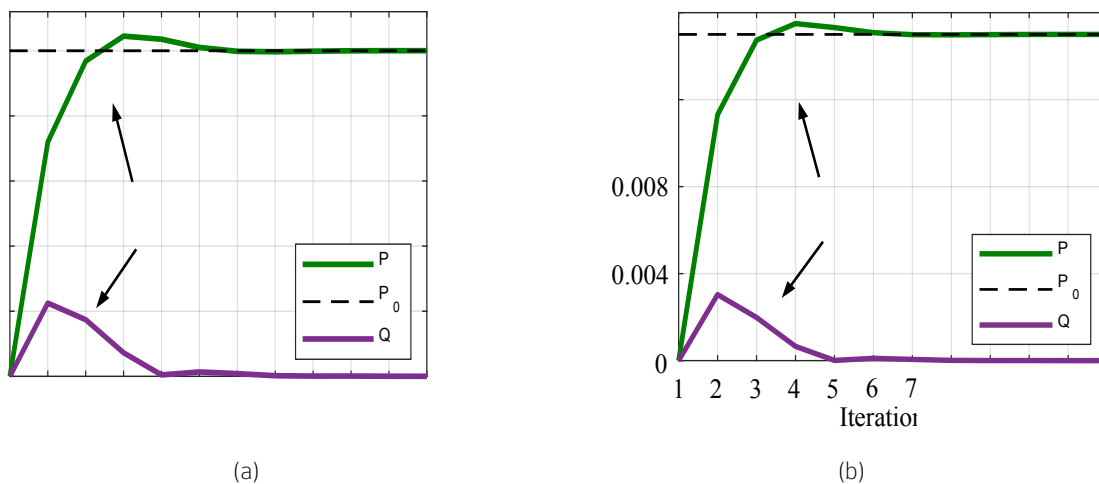
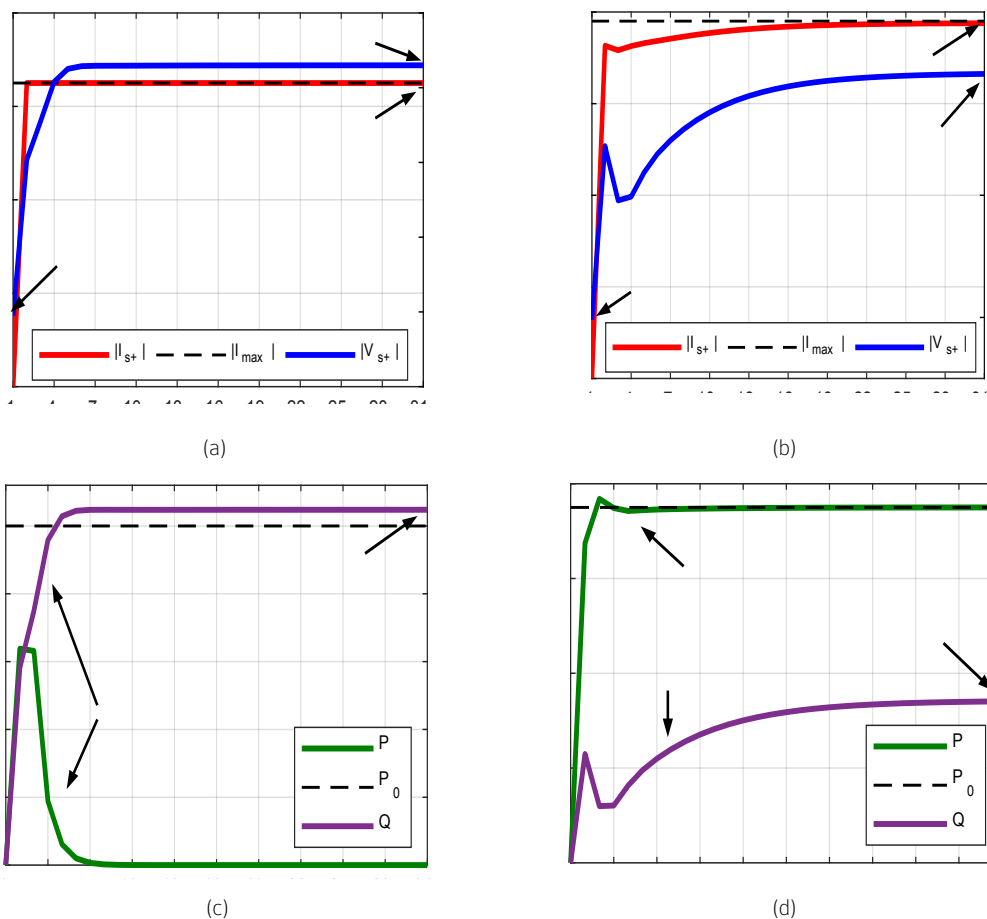


Figure 9 – LL (100 ) fault at bus 6: WT (a) and PV (b) positive sequence current contributions and feedback bus voltages; WT (c) and PV (d) active and reactive power injections.



As a different scenario, the converters' steady-state responses for the LL fault at bus 6 are also discussed. In this case, the feedback bus voltages for both PV and WT were low enough to enable FRT control. Figure 9 presents the positive sequence current contributions, the feedback bus voltages, and active and reactive power injections during the iterative process.

Figure 9a shows that, with the FRT mode enabled, the WT feedback voltage increases from  $0.7390\angle -0.7143^\circ$  pu (first iteration without voltage support) to  $0.8060\angle -1.1553^\circ$  pu, that corresponding to a voltage boost of 9.0663% in magnitude. Moreover, it is noted that the magnitude of the WT SC current contribution is restricted to its maximum value in order to protect the converter. For the PV, Figure 9b shows that the reactive current in positive sequence raises the voltage from  $0.8298\angle -0.4148^\circ$  pu (first iteration) to  $0.8500\angle -1.8079^\circ$  pu (upper limit of the FRT operation control for reactive consumption), which corresponds to a voltage boost of 2.4343% in magnitude.

As for the injected powers, it is noted in Figure 9c that the WT RFT control gives priority to reactive power injection by reducing the active power injection when the output current ( $|I_{S+}|$ ) reaches its maximum value (0.0325 pu). As the feedback voltage remains within the FRT control range, the active power is reduced to zero in order to provide voltage support to the grid by the reactive power injection. The iterative process achieves convergence with 31 iterations and results in the reactive power injection of 0.0262 pu.

In the PV case, Figure 9d shows that even in the FRT mode the injected active power is kept constant at its pre-fault value, i.e. 0.015 pu (after convergence). It is also noted that while the active power is kept constant, the FRT control adjusts the reactive power injection in order to provide voltage support. At the end of the iterative process, an injection of 0.0068 pu of reactive power is verified, which corresponds to a power factor of 0.9104 inductive.

The obtained results for the application example of the iterative approach demonstrate that it is possible to estimate the converter-controlled units SC current contribution in the steady-state short-circuit calculation without using time-domain simulations since the converter' steady-state response is defined by the grid requirements, i.e. its independent of the converter pre-fault control strategy or physical behavior of the PGU.

## 5 Conclusions

The increasing integration of distributed generation sources connected to the grid through power electronics converters has created with it the need to development of new methods for steady-state short-circuit calculating since the controlled nature of the fault current contributions from converters cannot be correctly addressed in the classical methods of SC calculation.

In this paper, a detailed iterative method is proposed for the steady-state fault analysis in power systems with distributed generation sources connected to the grid through converters. The proposed approach allows evaluating the steady-state current contribution from converters for symmetric and asymmetric faults considering the specifically required behavior in the electrical grid codes. As compared with time-domain simulations, the proposed approach has the advantage of requiring easily accessible converter' data to planning engineers and fast implementation and execution.

As a demonstration example, the proposed iterative method is used to calculate LG, LL, LLL, LLLG and LLLLG faults in a 17-bus test system containing PV and Type IV wind generators submitted to the Brazilian Electric Grid code requirements. By comparing the obtained results with the grid code requirements, the effectiveness of the proposed iterative approach in the estimation of the steady-state SC current contribution from converters is verified.

Therefore, for analysis of large and complex power system systems, the proposed iterative approach can be implemented as a complementary routine that runs at each iteration of the SC calculation tools of commercial power system analysis packages.

## ACKNOWLEDGEMENT

This work was conducted during a scholarship financed by CAPES – Brazilian Federal Agency for Support and Evaluation of Graduate Education within the Ministry of Education of Brazil.

## APPENDIX

The 17-bus test system data are presented in the following Tables I, II and III. All conductors have the same X/R ratio of 10 and their impedances are in the per-unit base of 100MVA. The transformer's reactance

is expressed as a percentage in their respective rated MVA.

**Table I – Conductors impedance in pu**

From	To	$X_{S+}$ (pu)	$X_{S0}$ (pu)
2	3	0.40	0.80
2	5	0.43	0.80
2	6	0.60	1.00
3	4	0.40	0.80
3	6	0.40	0.80
4	6	0.60	1.00
4	9	0.70	1.10
5	7	0.43	0.80
6	8	0.48	0.95
8	9	0.50	0.90
7	8	0.50	0.90
12	13	0.10	0.30
15	16	0.10	0.30

Source: authors.

**Table II – Transformers reactance**

HV bus	LV bus	(%)	LV side voltage (kV)	HV side voltage (kV)	Rated power (MVA)
1	2	10	34.5	230	100
10	4	10	34.5	230	100
11	7	10	34.5	230	100
12	9	10	34.5	230	100
15	5	10	34.5	230	100
14	13	7	0.6	34.5	5
17	16	7	0.6	34.5	5

Source: authors.

**Table III – PV and WT ratings**

	Rated power (MVA)	Rated voltage (kV)	Rated current (A)	Max. SC current (A)
WT	2.5	0.6	2406	3128
PV	1.5	0.6	1443	1876

Source: authors.

## REFERENCES

ABDALRAHMAN, A.; ZEKRY, A.; ALSHAZLY, A. Simulation and implementation of grid-connected

inverters. **International Journal of Computer Applications**, v. 60, n. 4, p. 41-49, 2012.

ANDERSON, P. M. **Analysis of faulted power systems**. New York: IEEE press, 1995.

BARSCHE, J. *et al.* Fault current contributions from wind plants. **A Report to the Transmission & Distribution Committee, Electric Machinery Committee and Power System Relaying Committee of the IEEE Power and Energy Society**, 2012.

BOLLEN, M. H. J.; HASSAN, F. **Integration of distributed generation in the power system**. Wiley, 2011.

CHEN, S. *et al.* Short-circuit calculations considering converter-controlled generation components. In: 2012 IEEE Energytech. Cleveland (United States), **Proceedings...** 2012. p. 1-6.

FISCHER, M.; MENDONÇA, A. Representation of variable speed full conversion wind energy converters for steady state short-circuit calculations. In: PES T&D 2012. Orlando (United States), **Proceedings...** 2012. p. 1-7.

GÖKSU, Ömer *et al.* An iterative approach for symmetrical and asymmetrical short-circuit calculations with converter-based connected renewable energy sources. Application to wind power. In: 2012 IEEE POWER AND ENERGY SOCIETY GENERAL MEETING. San Diego (United States), **Proceedings...** 2012. p. 1-8.

JENKINS, N.; EKANAYKE, J.; STRBAC, G. **Distributed generation**. The Institution of Engineering and Technology, 2010.

KAUFFMANN, T. *et al.* Phasor domain modeling of Type III wind turbine generator for protection studies. In: 2015 IEEE POWER & ENERGY SOCIETY GENERAL MEETING. Denver (United States), **Proceedings...** 2015. p. 1-5.

MOURA, A. P. *et al.* IMICV fault analysis method with multiple PV grid-connected inverters for distribution systems. **Electric Power Systems Research**, v. 119, p. 119-125, 2015.

NELSON, R. J. Short-circuit contributions of full converter wind turbines. In: PES T&D 2012. Orlando (United States), **Proceedings...** 2012. p. 1-5.

OPERADOR NACIONAL DO SISTEMA ELÉTRICO. **Submódulo 3.6: requisitos técnicos mínimos para a conexão às instalações de transmissão**,

revisão 2019.08, in portuguese. Available at:  
<<https://bit.ly/309g9aZ>>. Accessed: dec., 2019.

PLET, C. A. *et al.* Fault response of grid-connected inverter dominated networks. In: IEEE PES GENERAL MEETING. Providence (United States), **Proceedings...** 2010. p. 1-8.

TLEIS, N. **Power systems modelling and fault analysis: theory and practice**. Elsevier, 2007.

VALENTINI, M. *et al.* Fault current contribution from VSC-based wind turbines to the grid. In: 2nd INTERNATIONAL SYMPOSIUM ON ELECTRICAL AND ELECTRONICS ENGINEERING (ISEEE). Galati (Romania), **Proceedings...** 2008.

VAN DE SANDT, R. *et al.* Neutral earthing in offshore wind farm grids. In: 2009 IEEE BUCHAREST POWERTECH. Bucharest (Romania), **Proceedings...** 2009. p. 1-8.

WALLING, R. A.; GURSOY, E.; ENGLISH, B. Current contributions from Type 3 and Type 4 wind turbine generators during faults. In: PES T&D 2012. Orlando (United States), **Proceedings...** 2012. p. 1-6.